

Formal [2 + 2 + 2] Cycloaddition Reaction of a Metal–Carbyne Complex with Nitriles: Synthesis of a Metallapyrazine Complex

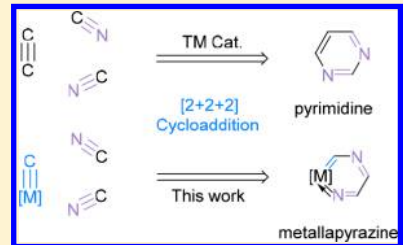
Jianfeng Lin,[†] Linting Ding,[†] Qingde Zhuo,[†] Hong Zhang,^{*,†,ID} and Haiping Xia^{*,†,‡,ID}

[†]State Key Laboratory of Physical Chemistry of Solid Surfaces and Collaborative Innovation Center of Chemistry for Energy Materials (iChEM), College of Chemistry and Chemical Engineering, Xiamen University, Xiamen 361005, China

[‡]Department of Chemistry, Shenzhen Grubbs Institute, Southern University of Science and Technology, Shenzhen 518055, China

Supporting Information

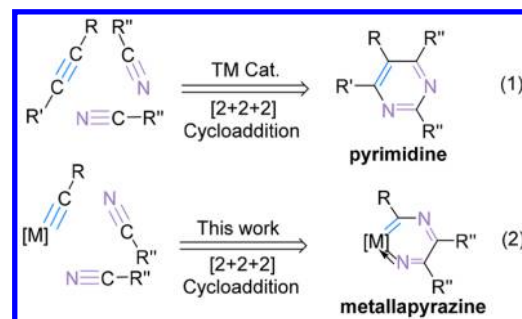
ABSTRACT: Although alkynes have been extensively exploited in [2 + 2 + 2] cycloadditions with nitriles to form N-heterocyclic aromatics, the “alkyne-like” metal–carbon triple bond has never been used in [2 + 2 + 2] cycloadditions with nitriles. We demonstrate the synthesis of the first metallapyrazine through [2 + 2 + 2] cycloaddition reactions of a metal–carbyne complex with nitriles. Experimental observations and density functional theory calculations are evidence for the aromatic character of the metallapentalenopyrazine.



INTRODUCTION

Transition-metal-catalyzed [2 + 2 + 2] cycloadditions have gained considerable popularity as efficient synthesis strategies to construct six-membered carbocycles, such as benzenes and cyclohexadienes, or heterocycles, such as pyridines and pyrimidines.¹ Alkynes and nitriles are two common structures containing triple bonds and are employed in [2 + 2 + 2] cycloadditions, which have been extensively studied with many catalysts.² The close structural relationship between alkynes with their carbon–carbon triple bonds and metal–carbyne complexes which contain metal–carbon triple bonds has inspired many attempts to investigate the reactivity similarities between these two moieties.³ The use of metal–carbyne species in the [2 + 2 + 2] cycloadditions with nitriles, however, remains elusive. Recently, we reported mettallapentalynes, a novel class of cyclic metal–carbyne complexes, which contain the smallest angles observed so far at a carbyne carbon and exhibit unusual planar Möbius aromaticity.⁴ The extremely strained bond angles of mettallapentalynes result in high reactivities, leading to cycloaddition reactions with various unsaturated substrates to produce a series of unique mettallacycles.⁵ Inspired by the [2 + 2 + 2] cycloadditions of alkynes and nitriles (Scheme 1, eq 1), we speculated that the metal–carbon triple bond within mettallacycles could be utilized as an excellent building block that, upon [2 + 2 + 2] cycloaddition reaction with nitriles, would lead to a metallapyrazine, a new cyclic structure (Scheme 1, eq 2). Here, we report a straightforward strategy, based on this hypothesis, to produce the first aromatic compounds with a metallapyrazine skeleton. Our strategy also provides convenient and regioselective access to extraordinary metal bridgehead aromatics with a high degree of skeletal complexity.

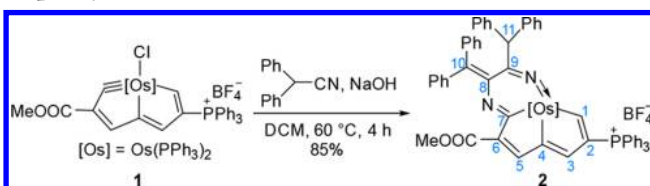
Scheme 1. Formal [2 + 2 + 2] Cycloaddition Reaction of a Metal–Carbyne Complex with Nitriles (TM Cat. = Transition Metal Catalysts)



RESULTS AND DISCUSSION

As shown in Scheme 2, treatment of osmapentalyne (1) with 2,2-diphenylacetonitrile in the presence of NaOH at 60 °C for 4 h led to a tricyclic complex (2) in 85% isolated yield. The structure of complex 2 was characterized by multinuclear magnetic resonance (NMR) spectroscopy, high-resolution

Scheme 2. Reaction of Osmapentalyne 1 with 2,2-Diphenylacetonitrile



Received: March 28, 2019

Published: May 2, 2019

mass spectrometry (HRMS), and elemental analysis (EA). The ¹H NMR spectrum of complex **2** showed a characteristic H1 signal at 11.46 ppm as a doublet split by the interaction with the phosphorus atom. Other protons of the metallacycle were observed at 6.86 (H5) and 5.96 (H3) ppm. In the ¹³C NMR spectrum, the characteristic signals of the metallacycle were observed at 226.74 (C1), 184.39 (C4), 182.65 (C7), 152.27 (C5), 147.98 (C6), 144.13 (C9), 141.30 (C8), 137.55 (C3), and 124.44 (C2) ppm.

The structure of **2** was verified by single-crystal X-ray crystallography. The crystal structure of **2-BPh₄**, the derivative of **2** with the counteranion BPh₄⁻ (Figure 1), reveals a six-

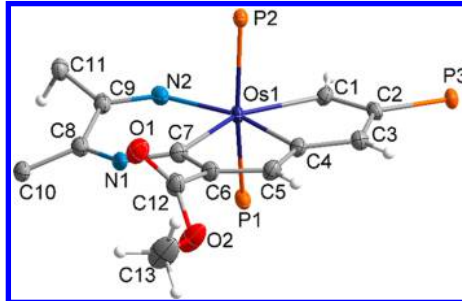
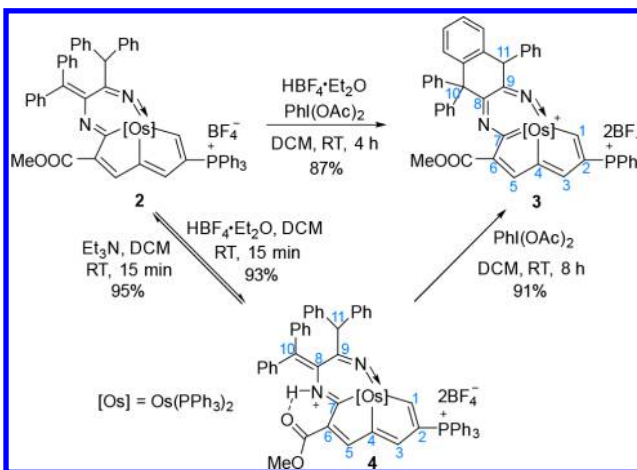


Figure 1. X-ray molecular structure for the cation of complex **2-BPh₄** drawn at the 50% probability level. The phenyl groups are omitted for clarity. Selected bond lengths (Å) and angles (deg): Os1–C1 2.075(3), Os1–C4 2.097(3), Os1–C7 2.135(3), Os1–N2 1.894(3), C1–C2 1.354(4), C2–C3 1.454(4), C3–C4 1.369(4), C4–C5 1.436(4), C5–C6 1.353(4), C6–C7 1.443(4), C7–N1 1.306(4), N1–C8 1.375(4), C8–C10 1.383(4), C8–C9 1.517(4), C9–N2 1.278(4); Os1–C1–C2 121.3(2), C1–C2–C3 112.7(3), C2–C3–C4 112.3(3), C3–C4–Os1 120.1(2), C4–Os1–C1 73.52(11), Os1–C4–C5 117.0(2), C4–C5–C6 115.0(3), C5–C6–C7 116.8(3), C6–C7–Os1 114.3(2), C7–Os1–C4 76.15(11), Os1–C7–N1 127.6(2), C7–N1–C8 129.1(3), N1–C8–C9 118.0(3), C8–C9–N2 116.4(3), C9–N2–Os1 145.9(2), N2–Os1–C7 80.22(11).

membered N-containing heterocycle fused to the original metallabicycle of **1**. The Os1–N2 and C9–N2 bond lengths of 1.894 and 1.278 Å, respectively, show that N2 is involved in a double bond⁶ in a six-membered osmapyrazine. The bond lengths of C7–N1 (1.306 Å) and C8–C10 (1.383 Å) suggest that they are conjugate double bonds, and the C–C bond lengths (C1–C2 1.354, C2–C3 1.454, C3–C4 1.369, C4–C5 1.436, C5–C6 1.353, C6–C7 1.443 Å) suggest that the fused five-membered rings are not π -electron delocalized.

As hypervalent iodine reagents are extensively used as oxidants in organic synthesis,⁷ complex **2** was allowed to react with a number of hypervalent iodine compounds with the hope to obtain the aromatic product by oxidative aromatization. Optimization of the conditions showed that the reaction of complex **2** with PhI(OAc)₂ in the presence of HBF₄ at room temperature for 4 h led to the formation in 87% isolated yield of an aromatic metallapyrazine derivative (**3**) (Scheme 3), which was characterized by NMR spectroscopy. In the ¹H NMR spectrum of **3**, characteristic signals are observed at 13.31 (H1), 9.47 (H5), and 8.59 (H3) ppm, downshifted significantly from the signals of complex **2**. The ¹³C NMR signals of the metallacycle also show downfield shifts and are observed at 240.84 (C1), 224.44 (C7), 195.69 (C4), 167.28 (C8), 166.65 (C5), 160.33 (C6), 150.25 (C3), 145.04 (C9), and 126.54 (C2) ppm. All of these chemical shifts indicate the aromatic character of **3**.

Scheme 3. Synthesis of the Metallapentalenopyrazine **3**



The structure of complex **3** was further confirmed by X-ray crystallography. As shown in Figure 2, the osmium atom of

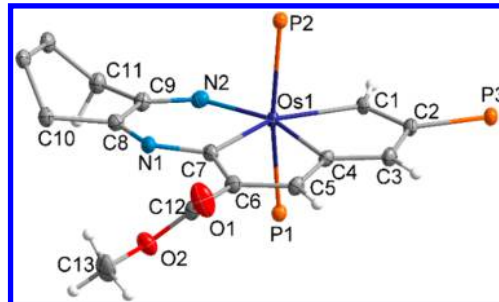


Figure 2. X-ray molecular structure for the cation of complex **3** drawn at the 50% probability level. The phenyl groups are omitted for clarity. Selected bond lengths (Å) and angles (deg): Os1–C1 2.068(2), Os1–C4 2.110(2), Os1–C7 2.067(2), Os1–N2 1.882(2), C1–C2 1.373(3), C2–C3 1.428(3), C3–C4 1.382(3), C4–C5 1.393(3), C5–C6 1.384(3), C6–C7 1.414(3), C7–N1 1.367(3), N1–C8 1.277(3), C8–C9 1.493(3), C9–N2 1.263(3); Os1–C1–C2 121.19(17), C1–C2–C3 113.1(2), C2–C3–C4 112.6(2), C3–C4–Os1 119.57(16), C4–Os1–C1 73.47(9), Os1–C4–C5 118.14(16), C4–C5–C6 114.2(2), C5–C6–C7 114.1(2), C6–C7–Os1 118.82(16), C7–Os1–C4 74.66(9), Os1–C7–N1 126.71(16), C7–N1–C8 127.1(2), N1–C8–C9 114.1(2), C8–C9–N2 116.0(2), C9–N2–Os1 144.43(17), N2–Os1–C7 82.28(9).

complex **3** is in a tricyclic framework. The tricyclic rings are nearly coplanar, as indicated by the small mean deviation of 0.065 Å from the least-squares plane. The C–C bond lengths of the fused five-membered rings (C1–C2 1.373, C2–C3 1.428, C3–C4 1.382, C4–C5 1.393, C5–C6 1.384, and C6–C7 1.414 Å) are almost equal and are intermediate between the bond lengths of typical C=C and C–C bonds. All of the Os–C bond lengths in complex **3** (Os1–C1 2.068, Os1–C4 2.110, and Os1–C7 2.067 Å) are in the range of reported osmapentale complexes (1.926–2.175 Å).^{5b–d,8} The bond length of Os1–N2 is 1.882 Å, which is comparable to the bond length of reported Os–N double bonds.⁶ The bond lengths of N1–C8 (1.277 Å) and Cep9–N2 (1.263 Å) are typical of conjugated C–N double bonds. All of these data suggest a delocalized structure of complex **3**. Notably, the metallapentalenopyrazine complex (**3**) exhibits good thermal stability. A solid sample of complex **3** is stable in air at 140 °C for at least 3 h (see Table S1).

The past decades have witnessed remarkable advances in the chemistry of metalla-aromatics^{5d,9} and have produced a diverse array of new aromatic complexes that are distinct from their organic molecules, such as metallabenzene,^{9b} metallabenzyne,^{9a–g} and metallapyridine.^{9c,10} However, the metalla-aromatics that have been currently reported do not overlap entirely with the classical aromatic species, especially those with N-heterocyclic rings. In particular, fused-ring N-heterocyclic metalla-aromatics are rare compared to the monocyclic N-heterocyclic metalla-aromatics. To the best of our knowledge, complexes containing a fused metallapyrazine structure have not been reported to date.

The new six-membered ring in complex 3 can be formed by the reaction of a phenyl group with a C=C double bond through a typical aromatic electrophilic substitution. We speculate that N1 may be first protonated by HBF₄ to enhance the electrophilicity of the C=C double bond in the reaction, and we examined the reaction between complex 2 and HBF₄, which led immediately to the formation of complex 4 in 93% isolated yield. As expected, complex 4 could be converted into complex 3 by reaction with PhI(OAc)₂ in the absence of HBF₄, whereas treatment with Et₃N led to the conversion of 4 to complex 2.

Complex 4 was fully characterized by single-crystal X-ray crystallography, NMR, HRMS, and EA. As shown in Figure 3,

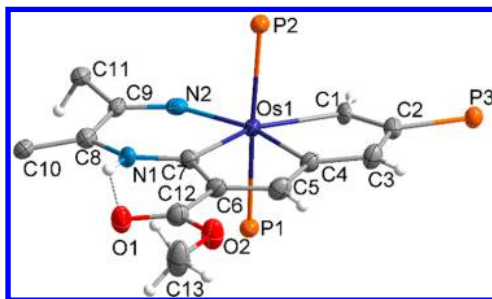


Figure 3. X-ray molecular structure for the cation of complex 4 drawn with 50% probability level. The phenyl groups are omitted for clarity. Selected bond lengths [Å] and angles [°]: Os1–C1 2.097(4), Os1–C4 2.088(4), Os1–C7 2.081(4), Os1–N2 1.878(3), C1–C2 1.358(6), C2–C3 1.444(6), C3–C4 1.349(6), C4–C5 1.422(6), C5–C6 1.366(6), C6–C7 1.458(6), C7–N1 1.328(5), N1–C8 1.413(5), C8–C10 1.370(6), C8–C9 1.491(6), C9–N2 1.283(5); Os1–C1–C2 119.5(3), C1–C2–C3 113.1(4), C2–C3–C4 113.4(4), C3–C4–Os1 120.0(3), C4–Os1–C1 73.79(16), Os1–C4–C5 116.9(3), C4–C5–C6 115.8(4), C5–C6–C7 114.2(4), C6–C7–Os1 116.5(3), C7–Os1–C4 76.58(16), Os1–C7–N1 126.6(3), C7–N1–C8 131.9(4), N1–C8–C9 115.3(3), C8–C9–N2 117.0(4), C9–N2–Os1 148.0(3), N2–Os1–C7 80.64(15).

the overall structural features of complex 4 is similar to complex 2, except the protonation of N1. There is strong hydrogen bonding interactions between N1H and O1, as indicated by the bond length of N1H–O1 (1.948 Å). In the ¹H NMR spectrum, the characteristic signal from H1 was observed at 12.29 ppm. The other down-shifted hydrogen signal (12.88 ppm) of complex 4 can be assigned to the NH. Other characteristic signals of metallacycles are observed at 8.48 (H5), 7.05 (H3) and 5.38 (H11) ppm, which are relatively downfield of those of complex 2. This is probably due to the electron-withdrawing effect of the NH⁺ group.

To shed light on the mechanism of the [2 + 2 + 2] cycloaddition reaction of the metal–carbyne complex 1 with

nitriles, other substituted nitriles were tested under the same reaction conditions. *In situ* NMR experiments suggest that complex 1 is unreactive toward 2-phenylpropanenitrile and acrylonitrile, and other aryl-substituted acetonitriles (such as 2-(pyridin-4-yl)acetonitrile and 2-phenylacetonitrile) can only undergo nucleophilic attack at C5 of the metallacycle in 1. We infer that the aryl groups may be an important stabilization contribution for the intermediate of the [2 + 2 + 2] cycloaddition reaction.

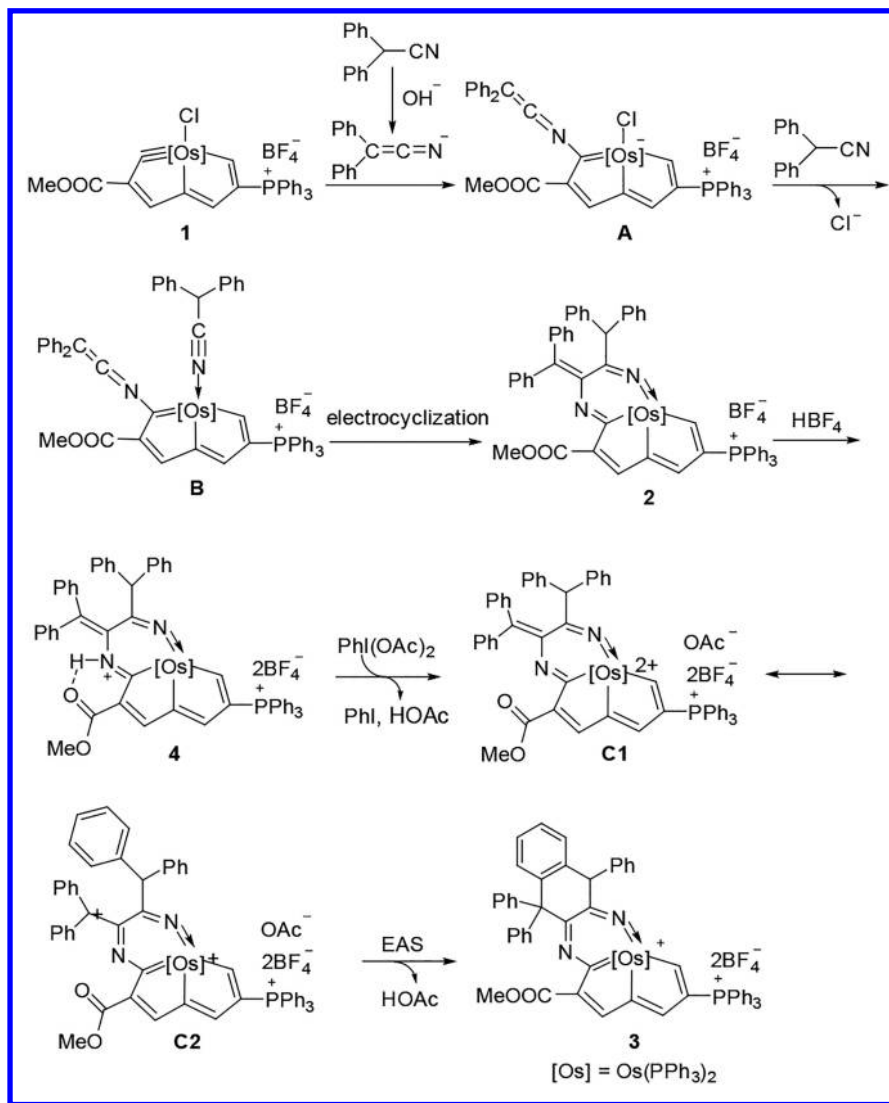
Based on the above experimental observations, a plausible mechanism can be proposed for the formation of metallapyrazine complex 3 and is shown in Scheme 4. According to the previous report,¹¹ the initial reaction of 2,2-diphenylacetone with sodium hydroxide may result in a ketenimine intermediate, which could nucleophilically attack the osmapentalyne 1 to form intermediate A. Similar nucleophilic addition reactions of the carbyne atom in metallapentalynes have been demonstrated.^{4b,d,5b,8a} Ligand substitution in A with another molecule of 2,2-diphenylacetone would afford B, which could facilitate the 6π electron cyclization reaction to produce complex 2. Evidence for the participation of the ketenimine intermediate could be derived from the experimental observation that no reaction occurs in the absence of sodium hydroxide. Subsequent protonation of 2 leads to the formation of complex 4, which could be oxidized by hypervalent iodine compound PhI(OAc)₂ to form intermediate C. The structure of C can be rationalized in terms of two resonance structures, C1 and C2, suggesting the high electrophilicity of the exocyclic double bond. The electrophilic aromatic substitution reaction of one of the phenyl rings by the exocyclic double bond could yield the final product 3.

The good thermal stability, downfield NMR signals, and equalized bond lengths, together with the ring planarity, are all consistent with the aromaticity of complex 3, which was investigated further by density functional theory calculations. Nucleus-independent chemical shifts (NICS) are commonly used as criteria to diagnose aromaticity.¹² The values of NICS(1)_{zz} of the model complex 3' (PH₃ groups were used to replace the PPh₃ ligands of complex 3) are shown in Figure 4A. The negative NICS values are similar to the reported values from metalla-aromatics,^{4a–c,8a–c,e} suggesting the aromatic character of the three metallacycles in the metallapentalenopyrazine 3. Note that the NICS(1)_{zz} value of ring A is obviously larger than those of ring B and ring C. A similar tendency has been demonstrated in our previously reported fused metalla-aromatics.^{8a–c} The reduced values of ring B and ring C may be ascribed to the adjacent two fused rings, which may decrease the aromaticity of ring B and ring C in comparison to ring A. Additionally, analysis of the anisotropy of the induced current density (ACID) provides a visual means of determining aromaticity.¹³ As shown in Figure 4B, the clockwise ring currents revealed in the ACID analysis further confirmed the aromaticity of complex 3. Isomerization stabilization energy (ISE)¹⁴ is another important criterion with which to explore aromaticity, in which energy increases when the conjugated bonds in the aromatic ring are interrupted. As shown in Figure 4C, the negative ISE values are comparable to those of an aromatic osmapentalene.^{4a,b,5a,8a–e}

CONCLUSION

In conclusion, we have exploited the formal [2 + 2 + 2] cycloaddition reaction of a metal–carbyne triple bond with

Scheme 4. Proposed Mechanism for the Formation of 3



nitriles as a new strategy for the synthesis of the first metallapentalenopyrazine motif. The resulting metallapentalenopyrazine 3 represents a novel N-heterocyclic species in a fused-ring metalla-aromatic system. Our combined experimental and computational studies have demonstrated the aromaticity of metallapentalenopyrazine 3. This approach not only extends the range of the classical [2 + 2 + 2] cycloaddition reaction but also offers insight into a strategy to construct previously inaccessible N-containing metalla-aromatic skeletons with congested metal centers.

EXPERIMENTAL SECTION

General Methods. All syntheses were carried out under an inert atmosphere (N_2) using standard Schlenk techniques unless otherwise stated. Solvents were distilled under N_2 from sodium/benzophenone (diethyl ether) or calcium hydride (dichloromethane). Complex 1 was synthesized according to published literature.¹ Other reagents were used as received from commercial sources without further purification. Column chromatography was performed on alumina gel (200–300 mesh) or silica gel (200–300 mesh) in air. Nuclear magnetic resonance spectroscopic experiments were performed on a Bruker AVIII-600 (^1H , 600.1 MHz; ^{13}C , 150.9 MHz; ^{31}P , 242.9 MHz) spectrometer at room temperature. ^1H and ^{13}C NMR chemical shifts are relative to tetramethylsilane, and ^{31}P NMR chemical shifts

are relative to 85% H_3PO_4 . The absolute values of the coupling constants are given in hertz (Hz). Multiplicities are abbreviated as singlet (s), doublet (d), triplet (t), multiplet (m), and broad (br). High-resolution mass spectra experiments were recorded on a Bruker En Apex Ultra 7.0T FT-MS. Elemental analyses were performed on a Vario EL III elemental analyzer.

Preparation of Complex 2. Method A: A mixture of complex 1 (500 mg, 0.40 mmol), 2,2-diphenylacetonitrile (232 mg, 1.2 mmol), and NaOH (16 mg, 0.40 mmol) in dichloromethane (15 mL) was stirred at 60 °C for 4 h to give a brown solution. Excess sodium salt was removed by filtration. The filtrate was evaporated under vacuum to a volume of ca. 2 mL, and then diethyl ether (20 mL) was added to the solution. The brown precipitate was collected by filtration, washed with diethyl ether (2 × 5 mL), and dried under vacuum to give complex 2 (543 mg, 85%). **Method B:** A mixture of 4 (200 mg, 0.12 mmol) and triethylamine (50 μL , 0.36 mmol) in dichloromethane (10 mL) was stirred at room temperature for 15 min to give a brown solution. The solution was evaporated under vacuum to a volume of ca. 2 mL, and then diethyl ether (15 mL) was added to the solution. The reddish-brown precipitate was collected by filtration, washed with diethyl ether (2 × 5 mL), and dried under vacuum to give 2 (182 mg, 95%). ^1H NMR plus $^1\text{H}-^{13}\text{C}$ HSQC (600.1 MHz, CD_2Cl_2) δ = 11.46 (d, $^3J(\text{H}, \text{P})$ = 19.3 Hz, 1H, H1), 7.75–5.96 (66H, Ph and H5), 6.86 (s, 1H, H5, confirmed by $^1\text{H}-^{13}\text{C}$ HSQC), 5.96 (s, 1H, H3), 5.08 (s, 1H, H11), 3.31 ppm (s, 3H, COOCH_3); ^{31}P NMR (242.9 MHz, CD_2Cl_2) δ = 12.19 (s, CPPh_3), -1.95 ppm (s, OsPPh_3); ^{13}C NMR

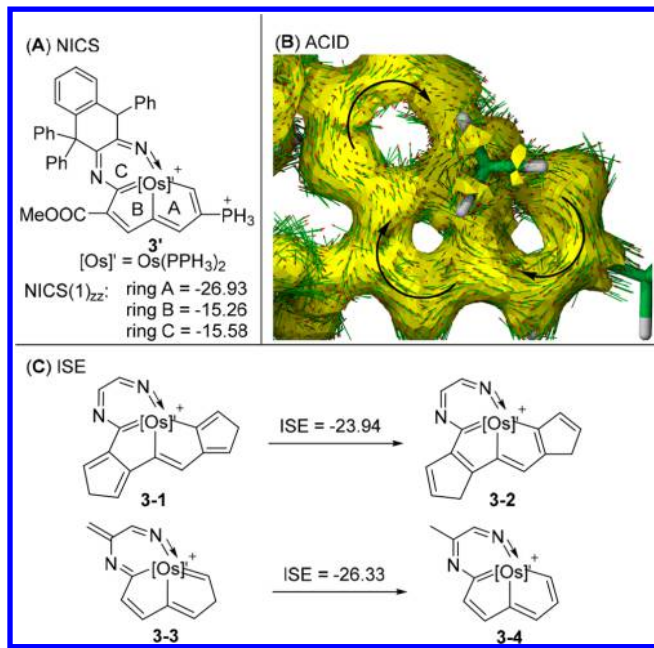


Figure 4. Evaluation of the aromaticity of 3. (A) NICS(1)_{zz} values (in ppm) at rings A, B, and C of model complex 3'. (B) ACID plot of model complex 3' with an isosurface value of 0.03. The magnetic field vector is orthogonal to the ring plane and is directed upward (aromatic species exhibit clockwise diatropic circulation). (C) Aromaticity of metallapentalenopyrazine evaluated by the ISE method (in kcal mol⁻¹). Calculated at the B3LYP functional with the LanL2DZ basis set for Os, P, and Cl and the 6-311++G(d,p) basis sets for C, N, and H, including zero-point energy corrections.

plus DEPT-135, HSQC, and HMBC (150.9 MHz, CD₂Cl₂) δ = 226.74 (m, C1), 184.39 (dt, ³J(C, P) = 14.0 Hz, ²J(C, P) = 5.3 Hz, C4), 182.65 (t, ²J(C, P) = 6.4 Hz, C7), 168.00 (s, COOCH₃), 152.27 (s, C5), 148.67 (Ph), 148.40 (Ph), 147.98 (t, ³J(C, P) = 3.6 Hz, C6), 144.43 (s, C10), 144.13 (s, C9), 141.30 (s, C8), 137.55 (d, ²J(C, P) = 23.6 Hz, C3), 135.64–126.61 (Ph), 124.44 (d, ¹J(C, P) = 67.9 Hz, C2), 121.06 (Ph), 120.47 (Ph), 52.28 (s, COOCH₃), 49.20 ppm (s, C11); HRMS (ESI) *m/z* calcd for [C₉H₇N₂O₂OsP₃]⁺, 1509.4416; found 1509.4407. Anal. Calcd (%) for C₉H₇BF₄N₂O₂OsP₃: C, 68.50; H, 4.55; N, 1.76. Found: C, 68.42; H, 4.95; N, 1.94

Preparation of Complex 2-BPh₄. A solution of NaBPh₄ (216 mg, 0.63 mmol) in MeOH (5 mL) was added to **2** (100 mg, 0.063 mmol) in DCM/MeOH (1 mL/2 mL). The reaction mixture was stirred for 2 min to give a brown suspension. The brown solid was collected by filtration, washed with MeOH (2 × 5 mL), and then dried under vacuum to give **2-BPh₄** (100 mg, 87%): ¹H NMR plus ¹H–¹³C HSQC (600.1 MHz, CD₂Cl₂) δ = 11.48 (d, ³J(H, P) = 19.4 Hz, 1H, H1), 7.70–6.00 (86H, Ph and H5), 6.92 (s, 1H, H5, confirmed by ¹H–¹³C HSQC), 5.98 (d, ³J(H, P) = 3.2 Hz, 1H, H3), 5.11 (s, 1H, H11), 3.35 ppm (s, 3H, COOCH₃); ³¹P NMR (242.9 MHz, CD₂Cl₂) δ = 12.19 (s, CPPh₃), -1.95 ppm (s, OsPPh₃); ¹³C NMR plus DEPT-135, HSQC, and HMBC (150.9 MHz, CD₂Cl₂) δ = 226.72 (m, C1), 184.43 (dt, ³J(C, P) = 23.9 Hz, ²J(C, P) = 5.3 Hz, C4), 182.62 (t, ²J(C, P) = 6.2 Hz, C7), 167.98 (s, COOCH₃), 165.34 (Ph), 165.01 (Ph), 164.69 (Ph), 164.36 (Ph), 152.24 (s, C5), 148.66 (Ph), 148.44 (Ph), 148.03 (t, ³J(C, P) = 3.5 Hz, C6), 144.42 (s, C10), 144.14 (s, C9), 141.28 (s, C8), 137.48 (d, ²J(C, P) = 24.8 Hz, C3), 135.67–126.40 (Ph), 124.36 (d, ¹J(C, P) = 67.2 Hz, C2), 121.03 (Ph), 120.47 (Ph), 52.29 (s, COOCH₃), 49.20 ppm (s, C11). Anal. Calcd (%) for C₁₁H₉BN₂O₂OsP₃: C, 75.56; H, 5.07; N, 1.53. Found: C, 75.29; H, 5.44; N, 1.82.

Preparation of Complex 3. Method A: A mixture of complex **2** (300 mg, 0.19 mmol), PhI(OAc)₂ (184 mg, 0.57 mmol), and HBF₄·Et₂O (151 μL, 0.57 mmol) in dichloromethane (10 mL) was stirred at room temperature for 4 h to give a gray solution. The solution was

evaporated under vacuum to a volume of ca. 2 mL, and then diethyl ether (20 mL) was added to the solution. The gray precipitate was collected by filtration, washed with diethyl ether (2 × 5 mL), and dried under vacuum to give complex **3** (278 mg, 87%). **Method B:** A mixture of complex **4** (300 mg, 0.18 mmol) and PhI(OAc)₂ (174 mg, 0.54 mmol) was stirred at room temperature for 8 h to give a gray solution. The solution was evaporated under vacuum to a volume of ca. 2 mL, and then diethyl ether (20 mL) was added to the solution. The gray precipitate was collected by filtration, washed with diethyl ether (2 × 5 mL), and dried under vacuum to give complex **3** (275 mg, 91%): ¹H NMR plus ¹H–¹³C HSQC (600.1 MHz, CD₂Cl₂) δ = 13.31 (m, 1H, H1), 9.47 (s, 1H, H5), 8.59 (d, 1H, ³J(H, P) = 3.8 Hz, H3), 7.84–6.25 ppm (64H, Ph), 5.44 (s, 1H, H11), 3.47 (s, 3H, COOCH₃); ³¹P NMR (242.9 MHz, CD₂Cl₂) δ = 16.27 (t, ⁴J(P, P) = 7.0 Hz, CPPh₃), 0.63 (dd, ²J(P, P) = 221.0 Hz, ⁴J(P, P) = 7.4 Hz, OsPPh₃), -11.06 ppm (dd, ²J(P, P) = 221.6 Hz, ⁴J(P, P) = 7.4 Hz, OsPPh₃); ¹³C NMR plus DEPT-135, HSQC, and HMBC (150.9 MHz, CD₂Cl₂) δ = 240.84 (m, C1), 224.44 (t, ²J(C, P) = 6.8 Hz, C7), 195.69 (d, ³J(C, P) = 23.4 Hz, C4), 167.28 (s, C8), 166.65 (s, C5), 165.38 (s, COOCH₃), 160.33 (t, ³J(C, P) = 3.5 Hz, C6), 150.25 (d, ²J(C, P) = 18.9 Hz, C3), 147.78 (Ph), 145.04 (s, C9), 142.04–117.80 (Ph), 126.54 (d, ¹J(C, P) = 53.4 Hz, C2), 64.15 (s, C10), 53.49 (s, COOCH₃), 48.13 ppm (s, C11); HRMS (ESI) *m/z* calcd for [C₉H₇N₂O₂OsP₃]²⁺, 754.2166; found 754.2196. Anal. Calcd (%) for C₉H₇B₂F₈N₂O₂OsP₃: C, 65.01; H, 4.26; N, 1.67. Found: C, 64.69; H, 4.60; N, 1.28.

Preparation of Complex 4. A solution of HBF₄·Et₂O (151 μL, 0.57 mmol) was added to a solution of complex **2** (300 mg, 0.19 mmol) in dichloromethane (10 mL). The reaction mixture was stirred at room temperature for 15 min to give a reddish-brown solution. The solution was evaporated under vacuum to a volume of ca. 2 mL, and then diethyl ether (20 mL) was added to the solution. The reddish-brown precipitate was collected by filtration, washed with diethyl ether (2 × 5 mL), and dried under vacuum to give complex **4** (297 mg, 93%): ¹H NMR plus ¹H–¹³C HSQC (600.1 MHz, CD₂Cl₂) δ = 12.88 (s, 1H, NH), 12.29 (d, ³J(H, P) = 17.7 Hz, 1H, H1), 8.48 (s, 1H, H5, confirmed by ¹H–¹³C HSQC), 7.82–5.93 (66H, Ph and H3), 7.05 (s, 1H, H3, confirmed by ¹H–¹³C HSQC), 5.38 (s, 1H, H11), 3.71 ppm (s, 3H, COOCH₃); ³¹P NMR (242.9 MHz, CD₂Cl₂) δ = 15.34 (s, CPPh₃), -1.30 ppm (s, OsPPh₃); ¹³C NMR plus DEPT-135, HSQC, and HMBC (150.9 MHz, CD₂Cl₂) δ = 233.81 (m, C1), 200.52 (t, ²J(C, P) = 6.5 Hz, C7), 181.88 (dt, ³J(C, P) = 23.5 Hz, ²J(C, P) = 4.1 Hz, C4), 166.59 (s, C5), 165.58 (s, COOCH₃), 152.26 (d, ²J(C, P) = 21.9 Hz, C3), 151.13 (Ph), 150.37 (s, C8), 141.31 (s, C10), 141.26 (s, C9), 137.73 (s, C6), 136.09–118.29 (Ph), 128.85 (d, ¹J(C, P) = 52.4 Hz, C2), 53.47 (s, COOCH₃), 49.80 ppm (s, C11); HRMS (ESI) *m/z* calcd for [C₉H₇N₂O₂OsP₃]²⁺, 755.2244; found 755.2279. Anal. Calcd (%) for C₉H₇B₂F₈N₂O₂OsP₃: C, 64.93; H, 4.37; N, 1.66. Found: C, 64.54; H, 4.27; N, 1.27.

Crystallographic Analysis. All single crystals suitable for X-ray diffraction were grown from a dichloromethane solution layered with hexane. Single-crystal X-ray diffraction data were collected on a Rigaku XtaLAB Synergy, Dualflex, HyPix diffractometer with mirror-monochromated Cu Kα radiation ($\lambda = 1.54184 \text{ \AA}$). The crystal was kept at 100.00 K during data collection. With Olex2,¹⁵ the structure was solved using the ShelXT¹⁶ structure solution program and refined with the ShelXL¹⁷ refinement package using least-squares minimization. Non-hydrogen atoms were refined anisotropically unless otherwise stated. Hydrogen atoms were introduced at their geometric positions and refined as riding atoms unless otherwise stated. CCDC-1899953 (**2-BPh₄**), CCDC-1899981 (**3**), and CCDC-1899955 (**4**) contain the supplementary crystallographic data for this paper. Some bad reflections of $(I_{\text{obs}} - I_{\text{cal}})/\sigma W > 10$ were omitted in **2-BPh₄**, **3**, and **4**. Water and a CH₂Cl₂ solvent in **4** were refined without hydrogen because of their disorder. These data can be obtained free of charge from the Cambridge Crystallographic Data Centre via www.ccdc.cam.ac.uk/data_request/cif.

Computational Details. All of the optimizations were performed with the Gaussian 09 software package.¹⁸ All structures were optimized at the B3LYP level of density functional theory.¹⁹ The

frequency calculations were performed to confirm the characteristics of the calculated structures as minima. In the B3LYP calculations, the effective core potentials of Hay and Wadt with a double- ξ valence basis set (LanL2DZ) were used to describe the Os and P, whereas the standard 6-311++G(d,p) basis set was used for all other atoms.²⁰ Polarization functions were added for Os ($z(f) = 0.886$) and P ($z(d) = 0.34$).²¹ The ACID calculations were carried out with the ACID program.²² Cartesian coordinates together with the symmetry and electronic energies for all the complexes were calculated in this study.

■ ASSOCIATED CONTENT

Supporting Information

The Supporting Information is available free of charge on the ACS Publications website at DOI: [10.1021/acs.organomet.9b00213](https://doi.org/10.1021/acs.organomet.9b00213).

Crystallographic data for complexes **2-BPh₄**, **3**, and **4** and copies of ¹H, ³¹P, and ¹³C NMR spectra of all new products (PDF)

Computed structures (XYZ)

Accession Codes

CCDC **1899953**, **1899955**, and **1899981** contain the supplementary crystallographic data for this paper. These data can be obtained free of charge via www.ccdc.cam.ac.uk/data_request/cif, or by emailing data_request@ccdc.cam.ac.uk, or by contacting The Cambridge Crystallographic Data Centre, 12 Union Road, Cambridge CB2 1EZ, UK; fax: +44 1223 336033.

■ AUTHOR INFORMATION

Corresponding Authors

*E-mail: zh@xmu.edu.cn.

*E-mail: hpxia@xmu.edu.cn.

ORCID

Hong Zhang: [0000-0003-3010-0806](https://orcid.org/0000-0003-3010-0806)

Haiping Xia: [0000-0002-2688-6634](https://orcid.org/0000-0002-2688-6634)

Notes

The authors declare no competing financial interest.

■ ACKNOWLEDGMENTS

This work was financially supported by the National Natural Science Foundation of China (U1705254, 21572185, and 21561162001).

■ REFERENCES

- (1) For selected reviews for [2 + 2 + 2] cycloaddition reactions, see: (a) Varela, J. A.; Saá, C. Construction of Pyridine Rings by Metal-Mediated [2 + 2 + 2] Cycloaddition. *Chem. Rev.* **2003**, *103*, 3787–3802. (b) Chopade, P. R.; Louie, J. [2 + 2 + 2] Cycloaddition Reactions Catalyzed by Transition Metal Complexes. *Adv. Synth. Catal.* **2006**, *348*, 2307–2327. (c) Heller, B.; Hapke, M. The fascinating construction of pyridine ring systems by transition metal-catalysed [2 + 2 + 2] cycloaddition reactions. *Chem. Soc. Rev.* **2007**, *36*, 1085–1094. (d) Domínguez, G.; Pérez-Castells, J. Recent advances in [2 + 2 + 2] cycloaddition reactions. *Chem. Soc. Rev.* **2011**, *40*, 3430–3444. (e) Shaaban, M. R.; El-Sayed, R.; Elwahy, A. H. M. Construction of fused heterocycles by metal-mediated [2 + 2 + 2] cyclotrimerization of alkynes and/or nitriles. *Tetrahedron* **2011**, *67*, 6095–6130. (f) Amatore, M.; Aubert, C. Recent Advances in Stereoselective [2 + 2 + 2] Cycloadditions. *Eur. J. Org. Chem.* **2015**, *2015*, 265–286. (g) Satoh, Y.; Obora, Y. Niobium Complexes in Organic Transformations: From Stoichiometric Reactions to Catalytic [2 + 2 + 2] Cycloaddition Reactions. *Eur. J. Org. Chem.* **2015**, *2015*, 5041–5054. (h) Hapke, M. Transition metal-free formal [2 + 2 + 2] cycloaddition reactions of alkynes. *Tetrahedron Lett.* **2016**, *57*, 5719–5729. (i) Lledó, A.; Pla-Quintana, A.; Roglans, A. Allenes, versatile unsaturated motifs in transition-metal-catalysed [2 + 2 + 2] cycloaddition reactions. *Chem. Soc. Rev.* **2016**, *45*, 2010–2023. (j) Babazadeh, M.; Soleimani-Amiri, S.; Vessally, E.; Hosseiniyan, A.; Edjlali, L. Transition metal-catalyzed [2 + 2 + 2] cycloaddition of nitrogen-linked 1,6-diynes: a straightforward route to fused pyrrolidine systems. *RSC Adv.* **2017**, *7*, 43716–43736. (k) Kotha, S.; Lahiri, K.; Sreevani, G. Design and Synthesis of Aromatics through [2 + 2 + 2] Cyclotrimerization. *Synlett* **2018**, *29*, 2342–2361. (l) Pla-Quintana, A.; Roglans, A. Chiral Induction in [2 + 2 + 2] Cycloaddition Reactions. *Asian J. Org. Chem.* **2018**, *7*, 1706–1718. (2) (a) Satoh, Y.; Yasuda, K.; Obora, Y. Strategy for the Synthesis of Pyrimidine Derivatives: NbCl₅-Mediated Cycloaddition of Alkynes and Nitriles. *Organometallics* **2012**, *31*, 5235–5238. (b) Satoh, Y.; Obora, Y. Low-Valent Niobium-Catalyzed Intermolecular [2 + 2 + 2] Cycloaddition of tert-Butylacetylene and Arylnitriles to Form 2,3,6-Trisubstituted Pyridine Derivatives. *J. Org. Chem.* **2013**, *78*, 7771–7776. (c) You, X.; Yu, S.; Liu, Y. Reactions of Zirconocene Butadiyne or Monoynne Complexes with Nitriles: Straightforward Synthesis of Functionalized Pyrimidines. *Organometallics* **2013**, *32*, 5273–5276. (d) Karad, S. N.; Liu, R.-S. Regiocontrolled Gold-Catalyzed [2 + 2 + 2] Cycloadditions of Ynamides with Two Discrete Nitriles to Construct 4-Aminopyrimidine Cores. *Angew. Chem., Int. Ed.* **2014**, *53*, 9072–9076. (e) Shintani, R.; Takagi, C.; Ito, T.; Naito, M.; Nozaki, K. Rhodium-Catalyzed Asymmetric Synthesis of Silicon-Stereogenic Dibenzosiloles by Enantioselective [2 + 2 + 2] Cycloaddition. *Angew. Chem., Int. Ed.* **2015**, *54*, 1616–1620. (f) Bednárová, E.; Colacino, E.; Lamaty, F.; Kotora, M. A Ruthenium Complex-Catalyzed Cyclotrimerization of Halogenated Alkynes with Nitriles. Synthesis of 2- and 3-Halopyridines. *Adv. Synth. Catal.* **2016**, *358*, 1916–1923. (g) Chen, Y.-L.; Sharma, P.; Liu, R.-S. Sulfonamide-directed gold-catalyzed 2 + 2 + 2 -cycloadditions of nitriles with two discrete ynamides to construct 2,4-diaminopyridine cores. *Chem. Commun.* **2016**, *52*, 3187–3190. (h) Ruhl, K. E.; Rovis, T. Visible light-gated cobalt catalysis for a spatially and temporally resolved [2 + 2 + 2] cycloaddition. *J. Am. Chem. Soc.* **2016**, *138*, 15527–15530. (i) You, X.; Xie, X.; Wang, G.; Xiong, M.; Sun, R.; Chen, H.; Liu, Y. Nickel-Catalyzed [2 + 2 + 2] Cycloaddition of Alkyne-Nitriles with Alkynes Assisted by Lewis Acids: Efficient Synthesis of Fused Pyridines. *Chem. - Eur. J.* **2016**, *22*, 16765–16769. (j) Fuji, M.; Obora, Y. FeCl₃-Assisted Niobium-Catalyzed Cycloaddition of Nitriles and Alkynes: Synthesis of Alkyl- and Arylpyrimidines Based on Independent Functions of NbCl₅ and FeCl₃ Lewis Acids. *Org. Lett.* **2017**, *19*, 5569–5572. (k) Wang, G.; You, X.; Gan, Y.; Liu, Y. Synthesis of δ - and α -Carbolines via Nickel-Catalyzed [2 + 2 + 2] Cycloaddition of Functionalized Alkyne-Nitriles with Alkynes. *Org. Lett.* **2017**, *19*, 110–113. (l) García-Lacuna, J.; Domínguez, G.; Blanco-Urgoiti, J.; Pérez-Castells, J. Cobalt Octacarbonyl-Catalyzed Scalable Alkyne Cyclotrimerization and Crossed [2 + 2 + 2]-Cycloaddition Reaction in a Plug Flow Reactor. *Org. Lett.* **2018**, *20*, 5219–5223. (m) Kiel, G. R.; Samkian, A. E.; Nicolay, A.; Witzke, R. J.; Tilley, T. D. Titanocene-Mediated Dinitrile Coupling: A Divergent Route to Nitrogen-Containing Polycyclic Aromatic Hydrocarbons. *J. Am. Chem. Soc.* **2018**, *140*, 2450–2454. (n) Low, C. H.; Rosenberg, J. N.; Lopez, M. A.; Agapie, T. Oxidative Coupling with Zr(IV) Supported by a Noninnocent Anthracene-Based Ligand: Application to the Catalytic Cotrimerization of Alkynes and Nitriles to Pyrimidines. *J. Am. Chem. Soc.* **2018**, *140*, 11906–11910. (o) Miura, H.; Tanaka, Y.; Nakahara, K.; Hachiya, Y.; Endo, K.; Shishido, T. Concerted Catalysis by Adjacent Palladium and Gold in Alloy Nanoparticles for the Versatile and Practical [2 + 2 + 2] Cycloaddition of Alkynes. *Angew. Chem., Int. Ed.* **2018**, *57*, 6136–6140. (3) (a) Buil, M. L.; Cardo, J. J. F.; Esteruelas, M. A.; Fernández, I.; Oñate, E. Hydroboration and Hydrogenation of an Osmium-Carbon Triple Bond: Osmium Chemistry of a Bis- σ -Borane. *Organometallics* **2015**, *34*, 547–550. (b) Kamitani, M.; Pinter, B.; Searles, K.; Crestani, M. G.; Hickey, A.; Manor, B. C.; Carroll, P. J.; Mindiola, D. J. Phosphinoalkylidene and -alkylidyne Complexes of Titanium:

- Intermolecular C–H Bond Activation and Dehydrogenation Reactions. *J. Am. Chem. Soc.* **2015**, *137*, 11872–11875. (c) Lackner, A. D.; Fürstner, A. The Triple-Bond Metathesis of Aryldiazonium Salts: A Prospect for Dinitrogen Cleavage. *Angew. Chem., Int. Ed.* **2015**, *54*, 12814–12818. (d) Buil, M. L.; Cardo, J. J. F.; Esteruelas, M. A.; Fernández, I.; Oñate, E. An Entry to Stable Mixed Phosphine-Osmium-NHC Polyhydrides. *Inorg. Chem.* **2016**, *55*, 5062–5070. (e) Buil, M. L.; Cardo, J. J. F.; Esteruelas, M. A.; Oñate, E. Dehydrogenative Addition of Aldehydes to a Mixed NHC-Osmium-Phosphine Hydroxide Complex: Formation of Carboxylate Derivatives. *Organometallics* **2016**, *35*, 2171–2173. (f) Buil, M. L.; Cardo, J. J. F.; Esteruelas, M. A.; Oñate, E. Square-Planar Alkylidyne–Osmium and Five-Coordinate Alkylidene–Osmium Complexes: Controlling the Transformation from Hydride-Alkylidyne to Alkylidene. *J. Am. Chem. Soc.* **2016**, *138*, 9720–9728. (g) Casanova, N.; Esteruelas, M. A.; Gulias, M.; Laramona, C.; Mascareñas, J. L.; Oñate, E. Amide-Directed Formation of Five-Coordinate Osmium Alkylidenes from Alkynes. *Organometallics* **2016**, *35*, 91–99. (h) Bukhryakov, K. V.; Schrock, R. R.; Hoveyda, A. H.; Tsay, C.; Müller, P. Syntheses of Molybdenum Oxo Alkylidene Complexes through Addition of Water to an Alkylidyne Complex. *J. Am. Chem. Soc.* **2018**, *140*, 2797–2800.
- (4) (a) Zhu, C.; Li, S.; Luo, M.; Zhou, X.; Niu, Y.; Lin, M.; Zhu, J.; Cao, Z.; Lu, X.; Wen, T.; Xie, Z.; Schleyer, P. v. R.; Xia, H. Stabilization of anti-aromatic and strained five-membered rings with a transition metal. *Nat. Chem.* **2013**, *5*, 698–703. (b) Zhu, C.; Luo, M.; Zhu, Q.; Zhu, J.; Schleyer, P. v. R.; Wu, J. I. C.; Lu, X.; Xia, H. Planar Möbius aromatic pentalenes incorporating 16 and 18 valence electron osmiums. *Nat. Commun.* **2014**, *5*, 3265. (c) Zhuo, Q.; Lin, J.; Hua, Y.; Zhou, X.; Shao, Y.; Chen, S.; Chen, Z.; Zhu, J.; Zhang, H.; Xia, H. Multiyne chains chelating osmium via three metal–carbon sigma bonds. *Nat. Commun.* **2017**, *8*, 1912. (d) Zhuo, Q.; Zhang, H.; Hua, Y.; Kang, H.; Zhou, X.; Lin, X.; Chen, Z.; Lin, J.; Zhuo, K.; Xia, H. Constraint of a ruthenium–carbon triple bond to a five-membered ring. *Sci. Adv.* **2018**, *4*, eaat0336.
- (5) (a) Zhu, C.; Yang, Y.; Luo, M.; Yang, C.; Wu, J.; Chen, L.; Liu, G.; Wen, T.; Zhu, J.; Xia, H. Stabilizing Two Classical Antiaromatic Frameworks: Demonstration of Photoacoustic Imaging and the Photothermal Effect in Metalla-aromatics. *Angew. Chem., Int. Ed.* **2015**, *54*, 6181–6185. (b) Luo, M.; Long, L.; Zhang, H.; Yang, Y.; Hua, Y.; Liu, G.; Lin, Z.; Xia, H. Reactions of Isocyanides with Metal Carbyne Complexes: Isolation and Characterization of Metallacycloprenimine Intermediates. *J. Am. Chem. Soc.* **2017**, *139*, 1822–1825. (c) Zhu, C.; Xia, H. Carboring Chemistry: A Story of Carbon Chain Ligands and Transition Metals. *Acc. Chem. Res.* **2018**, *51*, 1691–1700. (d) Zhu, C.; Zhu, J.; Zhou, X.; Zhu, Q.; Yang, Y.; Wen, T. B.; Xia, H. Isolation of an Eleven-Atom Polydentate Carbon-Chain Chelate Obtained by Cycloaddition of a Cyclic Osmium Carbyne with an Alkyne. *Angew. Chem., Int. Ed.* **2018**, *57*, 3154–3157.
- (6) (a) Brown, S. N. Oxidative Azavinylidene Formation in the Reaction of 1,3-Diphenylisobenzofuran with Osmium Nitride Complexes. *Inorg. Chem.* **2000**, *39*, 378–381. (b) Castarlenas, R.; Esteruelas, M. A.; Gutiérrez-Puebla, E.; Jean, Y.; Lledós, A.; Martín, M.; Oñate, E.; Tomàs, J. Synthesis, Characterization, and Theoretical Study of Stable Hydride–Azavinylidene Osmium(IV) Complexes. *Organometallics* **2000**, *19*, 3100–3108. (c) Castarlenas, R.; Esteruelas, M. A.; Gutiérrez-Puebla, E.; Oñate, E. Reactivity of the Imine–Vinylidene Complexes $\text{OsCl}_2(\text{CCHPh})(\text{NHCR}_2)(\text{PiPr}_3)_2$ [$\text{CR}_2 = \text{CMe}_2, \text{C}(\text{CH}_2)_4\text{CH}_2$]. *Organometallics* **2001**, *20*, 1545–1554. (d) Castarlenas, R.; Esteruelas, M. A.; Jean, Y.; Lledós, A.; Oñate, E.; Tomàs, J. Formation and Stereochemistry of Octahedral Cationic Hydride–Azavinylidene Osmium(IV) Complexes. *Eur. J. Inorg. Chem.* **2001**, *2001*, 2871–2883. (e) Castarlenas, R.; Esteruelas, M. A.; Oñate, E. One-Pot Synthesis for Osmium(II) Azavinylidene–Carbyne and Azavinylidene–Alkenylcarbyne Complexes Starting from an Osmium(II) Hydride–Azavinylidene Compound. *Organometallics* **2001**, *20*, 3283–3292. (f) Chen, J.; Huang, Z.-A.; Lu, Z.; Zhang, H.; Xia, H. Synthesis of Cyclic Vinylidene Complexes and Azavinylidene Complexes by Formal [4 + 2] Cyclization Reactions. *Chem. - Eur. J.* **2016**, *22*, 5363–5375.
- (7) (a) Zhdankin, V. V.; Stang, P. J. Chemistry of Polyvalent Iodine. *Chem. Rev.* **2008**, *108*, 5299–5358. (b) Yoshimura, A.; Zhdankin, V. V. Advances in Synthetic Applications of Hypervalent Iodine Compounds. *Chem. Rev.* **2016**, *116*, 3328–3435.
- (8) (a) Zhu, C.; Zhu, Q.; Fan, J.; Zhu, J.; He, X.; Cao, X.-Y.; Xia, H. A Metal-Bridged Tricyclic Aromatic System: Synthesis of Osmium Polycyclic Aromatic Complexes. *Angew. Chem., Int. Ed.* **2014**, *53*, 6232–6236. (b) Zhu, C.; Zhou, X.; Xing, H.; An, K.; Zhu, J.; Xia, H. σ -Aromaticity in an Unsaturated Ring: Osmapentalene Derivatives Containing a Metallacyclopene Unit. *Angew. Chem., Int. Ed.* **2015**, *54*, 3102–3106. (c) Zhu, C.; Yang, C.; Wang, Y.; Lin, G.; Yang, Y.; Wang, X.; Zhu, J.; Chen, X.; Lu, X.; Liu, G.; Xia, H. CCCCC pentadentate chelates with planar Möbius aromaticity and unique properties. *Sci. Adv.* **2016**, *2*, e1601031. (d) Zhu, C.; Wu, J.; Li, S.; Yang, Y.; Zhu, J.; Lu, X.; Xia, H. Synthesis and characterization of a metallacyclic framework with three fused five-membered rings. *Angew. Chem., Int. Ed.* **2017**, *56*, 9067–9071. (e) Zhou, X.; Wu, J.; Hao, Y.; Zhu, C.; Zhuo, Q.; Xia, H.; Zhu, J. Rational Design and Synthesis of Unsaturated Se-Containing Osmacycles with σ -Aromaticity. *Chem. - Eur. J.* **2018**, *24*, 2389–2395.
- (9) For reviews, see: (a) Jia, G. Progress in the Chemistry of Metallabenzenes. *Acc. Chem. Res.* **2004**, *37*, 479–486. (b) Landorf, C. W.; Haley, M. M. Recent Advances in Metallabenzenes Chemistry. *Angew. Chem., Int. Ed.* **2006**, *45*, 3914–3936. (c) Wright, L. J. Metallabenzenes and metallabenzenoids. *Dalton Transactions* **2006**, 1821–1827. (d) Bleeke, J. R. Aromatic Iridacycles. *Acc. Chem. Res.* **2007**, *40*, 1035–1047. (e) Jia, G. Recent progress in the chemistry of osmium carbyne and metallabenzyne complexes. *Coord. Chem. Rev.* **2007**, *251*, 2167–2187. (f) Panque, M.; Poveda, M. L.; Rendón, N. Synthesis and Reactivity of Iridacycles Containing the TpMe_2Ir Moiety. *Eur. J. Inorg. Chem.* **2011**, *2011*, 19–33. (g) Chen, J.; Jia, G. Recent development in the chemistry of transition metal-containing metallabenzenes and metallabenzenes. *Coord. Chem. Rev.* **2013**, *257*, 2491–2521. (h) Cao, X.-Y.; Zhao, Q.; Lin, Z.; Xia, H. The Chemistry of Aromatic Osmacycles. *Acc. Chem. Res.* **2014**, *47*, 341–354. (i) Frogley, B. J.; Wright, L. J. Fused-ring metallabenzenes. *Coord. Chem. Rev.* **2014**, *270*–*271*, 151–166. (j) Wei, J.; Zhang, W.-X.; Xi, Z. Dianions as Formal Oxidants: Synthesis and Characterization of Aromatic Dilithionickeloles from 1,4-Dilithio-1,3-butadienes and $[\text{Ni}(\text{cod})_2]$. *Angew. Chem., Int. Ed.* **2015**, *54*, 5999–6002. (k) Wei, J.; Zhang, Y.; Zhang, W.-X.; Xi, Z. 1,3-Butadienyl Dianions as Non-Innocent Ligands: Synthesis and Characterization of Aromatic Dilithio Rhodacycles. *Angew. Chem., Int. Ed.* **2015**, *54*, 9986–9990. (l) Wei, J.; Zhang, Y.; Chi, Y.; Liu, L.; Zhang, W.-X.; Xi, Z. Aromatic Dicupra[10]annulenes. *J. Am. Chem. Soc.* **2016**, *138*, 60–63. (m) Zhang, Y.; Chi, Y.; Wei, J.; Yang, Q.; Yang, Z.; Chen, H.; Yang, R.; Zhang, W.-X.; Xi, Z. Aromatic Tetralithiodigalloles with a Ga–Ga Bond: Synthesis and Structural Characterization. *Organometallics* **2017**, *36*, 2982–2986. (n) Zhang, Y.; Wei, J.; Chi, Y.; Zhang, X.; Zhang, W.-X.; Xi, Z. Spiro Metalla-aromatics of Pd, Pt, and Rh: Synthesis and Characterization. *J. Am. Chem. Soc.* **2017**, *139*, 5039–5042. (o) Frogley, B. J.; Wright, L. J. Recent Advances in Metallaaromatics. *Chem. - Eur. J.* **2018**, *24*, 2025–2038. (p) Wang, H.; Zhou, X.; Xia, H. Metallaaromatics Containing Main-group Heteroatoms. *Chin. J. Chem.* **2018**, *36*, 93–105. (q) Wei, J.; Zhang, W.-X.; Xi, Z. The aromatic dianion metalloles. *Chem. Sci.* **2018**, *9*, 560–568. (r) Zhang, Y.; Yang, Z.; Zhang, W.-X.; Xi, Z. Indacyclopentadienes and Aromatic Indacyclopentadienyl Dianions: Synthesis and Characterization. *Chem. - Eur. J.* **2019**, *25*, 4218–4224. (10) (a) Liu, B.; Wang, H.; Xie, H.; Zeng, B.; Chen, J.; Tao, J.; Wen, T. B.; Cao, Z.; Xia, H. Osmapyridine and Osmapyridinium from a Formal [4 + 2] Cycloaddition Reaction. *Angew. Chem., Int. Ed.* **2009**, *48*, 5430–5434. (b) Liu, B.; Zhao, Q.; Wang, H.; Chen, J.; Cao, X.; Cao, Z.; Xia, H. Synthesis of Osmapyridiniums by [4 + 2] Cycloaddition Reaction between Osmium Alkenylcarbyne and Nitriles. *Chin. J. Chem.* **2012**, *30*, 2158–2168. (11) (a) Newman, M. S.; Fukunaga, T.; Miwa, T. Alkylation of Nitriles: Ketenimine Formation. *J. Am. Chem. Soc.* **1960**, *82*, 873–875. (b) Trofimenko, S. Dicyanoketenimine (Cyanoform). *J. Org.*

- Chem.* **1963**, *28*, 217–218. (c) West, R.; Gornowicz, G. A. Polyliithium compounds. IV. Polylithiation of nitriles and the preparations of trisilyl ynamines. *J. Am. Chem. Soc.* **1971**, *93*, 1714–1720. (d) Watt, D. S. The Silylation of Nitrile Anions. Silylketenimines AU. *Synth. Commun.* **1974**, *4*, 127–131. (e) Cunico, R. F.; Kuan, C. P. The metalation-silylation of O-trimethylsilyl aldehyde cyanohydrins. *J. Org. Chem.* **1992**, *57*, 1202–1205. (f) Denmark, S. E.; Wilson, T. W. N-silyl oxyketene imines are underused yet highly versatile reagents for catalytic asymmetric synthesis. *Nat. Chem.* **2010**, *2*, 937–943. (g) Long, S.; Panunzio, M.; Qin, W.; Bongini, A.; Monari, M. Efficient Aldol-Type Reaction of O-Protected α -Hydroxy Aldehydes and N-Trimethylsilyl Ketene Imines: Synthesis of β,γ -Dihydroxy-Nitriles. *Eur. J. Org. Chem.* **2013**, *2013*, 5127–5142. (h) Qin, W.; Long, S.; Bongini, A.; Panunzio, M. α -Alkyl- α -aryl (Trimethyltin) Nitriles: Versatile Nucleophilic Intermediates in Aldol-Like Reactions. *Eur. J. Org. Chem.* **2015**, *2015*, 3495–3505. (i) Sasaki, M.; Ando, M.; Kawahata, M.; Yamaguchi, K.; Takeda, K. Spontaneous Oxygenation of Siloxy-N-silylketenimines to α -Ketoamides. *Org. Lett.* **2016**, *18*, 1598–1601.
- (12) (a) Schleyer, P. v. R.; Maerker, C.; Dransfeld, A.; Jiao, H.; van Eikema Hommes, N. J. R. Nucleus-Independent Chemical Shifts: A Simple and Efficient Aromaticity Probe. *J. Am. Chem. Soc.* **1996**, *118*, 6317–6318. (b) Schleyer, P. v. R.; Manoharan, M.; Wang, Z.-X.; Kiran, B.; Jiao, H.; Puchta, R.; van Eikema Hommes, N. J. R. Dissected Nucleus-Independent Chemical Shift Analysis of π -Aromaticity and Antiaromaticity. *Org. Lett.* **2001**, *3*, 2465–2468. (c) Chen, Z.; Wannere, C. S.; Corminboeuf, C.; Puchta, R.; Schleyer, P. v. R. Nucleus-Independent Chemical Shifts (NICS) as an Aromaticity Criterion. *Chem. Rev.* **2005**, *105*, 3842–3888. (d) Falalah-Bagher-Shaidei, H.; Wannere, C. S.; Corminboeuf, C.; Puchta, R.; Schleyer, P. v. R. Which NICS Aromaticity Index for Planar π Rings Is Best? *Org. Lett.* **2006**, *8*, 863–866.
- (13) (a) Herges, R.; Geuenich, D. Delocalization of Electrons in Molecules. *J. Phys. Chem. A* **2001**, *105*, 3214–3220. (b) Geuenich, D.; Hess, K.; Köhler, F.; Herges, R. Anisotropy of the Induced Current Density (ACID), a General Method to Quantify and Visualize Electronic Delocalization. *Chem. Rev.* **2005**, *105*, 3758–3772.
- (14) (a) Schleyer, P. v. R.; Pühlhofer, F. Recommendations for the Evaluation of Aromatic Stabilization Energies. *Org. Lett.* **2002**, *4*, 2873–2876. (b) Wannere, C. S.; Moran, D.; Allinger, N. L.; Hess, B. A.; Schaad, L. J.; Schleyer, P. v. R. On the Stability of Large [4n]Annulenes. *Org. Lett.* **2003**, *5*, 2983–2986. (c) Zhu, J.; An, K.; Schleyer, P. v. R. Evaluation of Triplet Aromaticity by the Isomerization Stabilization Energy. *Org. Lett.* **2013**, *15*, 2442–2445.
- (15) Dolomanov, O. V.; Bourhis, L. J.; Gildea, R. J.; Howard, J. A. K.; Puschmann, H. OLEX2: A Complete Structure Solution, Refinement and Analysis Program. *J. Appl. Crystallogr.* **2009**, *42*, 339–341.
- (16) Sheldrick, G. M. SHELXT-Integrated Space-Group and Crystal-Structure Determination. *Acta Crystallogr., Sect. A: Found. Adv.* **2015**, *A71*, 3–8.
- (17) Sheldrick, G. M. Crystal Structure Refinement with SHELXL. *Acta Crystallogr., Sect. C: Struct. Chem.* **2015**, *C71*, 3–8.
- (18) Frisch, M. J.; Trucks, G. W.; Schlegel, H. B.; Scuseria, G. E.; Robb, M. A.; Cheeseman, J. R.; Scalmani, G.; Barone, V.; Mennucci, B.; Petersson, G. A.; Nakatsuji, H.; Caricato, M.; Li, X.; Hratchian, H. P.; Izmaylov, A. F.; Bloino, J.; Zheng, G.; Sonnenberg, J. L.; Hada, M.; Ehara, M.; Toyota, K.; Fukuda, R.; Hasegawa, J.; Ishida, M.; Nakajima, T.; Honda, Y.; Kitao, O.; Nakai, H.; Vreven, T.; Montgomery, J. A., Jr.; Peralta, J. E.; Ogliaro, F.; Bearpark, M.; Heyd, J. J.; Brothers, E.; Kudin, K. N.; Staroverov, V. N.; Kobayashi, R.; Normand, J.; Raghavachari, K.; Rendell, A.; Burant, J. C.; Iyengar, S. S.; Tomasi, J.; Cossi, M.; Rega, N.; Millam, J. M.; Klene, M.; Knox, J. E.; Cross, J. B.; Bakken, V.; Adamo, C.; Jaramillo, J.; Gomperts, R.; Stratmann, R. E.; Yazyev, O.; Austin, A. J.; Cammi, R.; Pomelli, C.; Ochterski, J. W.; Martin, R. L.; Morokuma, K.; Zakrzewski, V. G.; Voth, G. A.; Salvador, P.; Dannenberg, J. J.; Dapprich, S.; Daniels, A. D.; Farkas, O.; Foresman, J. B.; Ortiz, J. V.; Cioslowski, J.; Fox, D. J. *Gaussian 09*, revision D. 01; Gaussian Inc.: Wallingford, CT, 2013.
- (19) (a) Lee, C.; Yang, W.; Parr, R. G. Development of the Colle-Salvetti Correlation-Energy Formula into a Functional of the Electron Density. *Phys. Rev. B: Condens. Matter Mater. Phys.* **1988**, *37*, 785–789. (b) Miehlich, B.; Savin, A.; Stoll, H.; Preuss, H. Results Obtained with the Correlation Energy Density Functionals of Becke and Lee, Yang and Parr. *Chem. Phys. Lett.* **1989**, *157*, 200–206. (c) Becke, A. D. Density-Functional Thermochemistry. III. The Role of Exact Exchange. *J. Chem. Phys.* **1993**, *98*, 5648–5652.
- (20) Hay, P. J.; Wadt, W. R. Ab Initio Effective Core Potentials for Molecular Calculations. Potentials for K to Au Including the Outermost Core Orbitals. *J. Chem. Phys.* **1985**, *82*, 299–310.
- (21) Huzinaga, S.; Andzelm, J.; Radzio-Andzelm, E.; Sakai, Y.; Tatewaki, H.; Klobukowski, M. *Gaussian Basis Sets for Molecular Calculations*; Elsevier Science Publishing: Amsterdam, 1984.
- (22) Geuenich, D.; Hess, K.; Köhler, F.; Herges, R. Anisotropy of the Induced Current Density (ACID), a General Method to Quantify and Visualize Electronic Delocalization. *Chem. Rev.* **2005**, *105*, 3758–3772.